



Partial characterization of the molecular nature of collagen-linked fluorescence: Role of diabetes and end-stage renal disease

David R. Sell^{a,*}, Ina Nemet^a, Vincent M. Monnier^{a,b}

^a Department of Pathology, Case Western Reserve University, Wolstein Research Bldg., 2103 Cornell Road, Cleveland, OH 44106-7288, USA

^b Department of Biochemistry, Case Western Reserve University, 10900 Euclid Avenue, Cleveland, OH 44106-4935, USA

ARTICLE INFO

Article history:

Received 15 September 2009
and in revised form 26 October 2009
Available online 30 October 2009

Keywords:

Aging
Glycation
Skin
Structure
Marker
Diabetes
Renal disease

ABSTRACT

Collagen-linked fluorescence at excitation/emission 370/440 nm has widely been used as a marker for advanced glycation in studies of aging, diabetic complications, and end-stage renal disease (ESRD). Diagnostic devices measuring skin autofluorescence at this wavelength revealed an association between fluorescence and cardiovascular morbidity and mortality. We now report the presence of a major fluorophore (LW-1) in human skin collagen which increases with age, diabetes, and ESRD. It has a molecular weight of 623.2 Da, a UV maximum at 348 nm, and involves a lysine residue in an aromatic ring. LW-1 could not be synthesized using traditional glycation chemistry suggesting a complex mechanism of formation, perhaps related to hypoxia since elevated levels were also found in nondiabetic individuals with chronic lung disease.

© 2009 Elsevier Inc. All rights reserved.

Introduction

Several years ago our laboratory introduced protein-linked fluorescence measured at excitation/emission 370/440 nm; i.e., long-wavelength fluorescence (LW)¹ as a putative and surrogate marker for the nonenzymatic browning reaction *in vivo*; the Maillard reaction [1]. We found that skin collagen-linked LW was strongly associated with the severity of retinopathy, nephropathy, arterial, and joint stiffness in type 1 diabetes [2]. In a DCCT ancillary study, we found that LW was not only associated with severity of microvascular disease [3], but was also associated with coronary calcium deposition [4]. Over the years, collagen-linked LW has been used in a large number of studies without challenge as to the nature of the molecular structure of the entities responsible for the fluorescence and its biological origin. Thus, although LW might be linked to glycation,

this fact has never been established. Recently, renewed interest into the chemical nature of LW has emerged for several reasons. First, there has been introduction onto the commercial market of diagnostic devices capable of noninvasively measuring LW in forearm skin of individuals at risk for diabetes and its complications [5–8]; i.e., the AGE Reader (DiagnOptics, Groningen, The Netherlands) and SCOUT DS (VeraLight, Albuquerque, NM). Second, studies with this device have shown a number of important associations between LW in skin vs. renal function and mortality in hemodialysis patients [9–11], vascular stiffness [12,13], coronary artery calcification [9], micro- and macrovascular complications of diabetes including nephropathy [8,9,14,15], neuropathy [8,9,15,16], and retinopathy [8].

For these reasons, we initiated work on the molecular nature of LW expecting to find a novel AGE product whose structure would be easily confirmed via total synthesis from collagen or amino acids incubated with reactive carbonyl compounds. Below we describe the isolation, purification, and partial molecular characterization of a single major protein-bound, acid-labile fluorophore (LW-1) whose levels are elevated by aging, diabetes, end-stage renal disease, and in selected people deceased from lung disease.

Materials and methods

Reagents

Except as noted, most chemicals and solvents were from Sigma–Aldrich or Fisher and were of the highest grade available. The

* Corresponding author. Address: Department of Pathology, Case Western Reserve University, Wolstein Research Bldg., 2103 Cornell Road, Cleveland, OH 44106-7288, USA. Fax +1 216 368 1357.

E-mail address: drs7@po.cwru.edu (D.R. Sell).

¹ Abbreviations used: CE, collision energy; CHF, congestive heart failure; CRD, chronic renal failure; DCCT, The Diabetes Complications and Control Trial; DTPA, diethylene triamine penta acetic acid; ESRD, end-stage renal disease; ex/em, excitation/emission (fluorescence maxima); HFBA, heptafluorobutyric acid; HSQC, heteronuclear single quantum coherence; Ir, long-range (NMR chemical coupling); LW, long-wavelength fluorescence; LW-1, long-wavelength collagen-linked fluorophore; MS, mass spectrometry; MRM, multiple reaction monitoring; RT, retention time; SRM, selected reaction monitoring; TFA, trifluoroacetic acid; TOCSY, total correlation spectroscopy.

advanced glycation end products K2P and ST29 were generously provided by Dr. B.J. Ortwerth (University of Missouri, Columbia, MO); argpyrimidine was from Dr. Marcus Glomb (Martin Luther University, Halle, Germany); ONE-pyrrole from Dr. Larry Sayre² (Case Western Reserve University, Cleveland, OH); and pentosidine was from IMARS (International Maillard Reaction Society, Cleveland, OH).

Tissue procurement and donor information

As previously described [17], human skin specimens were obtained at autopsy procured through the Tissue Procurement Facility at University Hospitals Case Medical Center (Cleveland, OH) or the National Disease Research Interchange (NDRI, Philadelphia, PA). All samples were stored frozen at -80°C . Skin donors used for LW-1 isolation procedures (Fig. 1) and quantitative analyses (Fig. 11) are listed in the [Supplementary material as Tables S1 and S2](#), respectively. LW-1 was isolated from $n = 8$ different skin samples from donors of age range 47 to 69 years, all with diabetes and $n = 6$ with either chronic renal failure (CRF) or end-stage renal disease (ESRD) (see [Supplement](#)). Diagnoses of diabetes and renal disease and other major pathologies including the cause of death were obtained from the medical and anatomical records of each patient at postmortem.

Preparation of insoluble skin collagen

Procedures have previously been described [17]. Briefly, the skin samples were defatted (2:1 chloroform–methanol), extracted (1 M sodium chloride and 0.5 M acetic acid), and digested (0.1% pepsin in 0.5 M acetic acid) at 4°C for 24 h each, and freeze-dried (Flexi-Dry, FTS, Stone Ridge, NY). To scale-up the procedure for LW-1 isolation, large strips of skin measuring $\approx 2 \times 10$ cm or smaller from $n = 8$ donors with diabetes and/or renal disease ([Supplement](#)) were extracted separately but with a combine wet weight of ≈ 75 g skin after removal of the epidermis and subcutaneous fat as previously described [17]. The yield of insoluble collagen for each of these samples after extraction and freeze-drying are shown in [Table S1 \(Supplement\)](#). Subsequently, these extracted samples were combined together for enzymatic digestion.

Enzymatic digestion of insoluble skin collagen

The protocol used for enzymatic digestion of insoluble collagen has previously been described [17]. Briefly, it involved the sequential digestion of insoluble collagen with a series of enzymes listed in [Fig. 1](#). For analytical assays, 5 mg of freeze-dried pellet of insoluble collagen for each sample was digested. For LW-1 purification, a scaled-up version of this protocol was used to digest ≈ 12 g insoluble collagen which yielded ≈ 435 ml of digest (see [Fig. 1](#)). The percent digestion was determined by hydroxyproline as previously described [17].

Overview of LW-1 purification procedures

LW-1 was purified using a large-batch protocol as outlined in [Fig. 1](#). The digest was desalted on a C18 column followed by repeated injections on HPLC as summarized in [Fig. 1](#). The isolate was submitted for UV, NMR, and mass spectrometry (MS) analyses.

Desalting

The digest was desalted using C18 10 g Sep-Pak columns (Waters Corporation, Milford, MA). Each column was washed with methanol and equilibrated with water/0.1% trifluoroacetic acid

(TFA) prior to loading ≈ 25 ml digest onto each of these columns. Each column was then washed with 50 ml of water/0.1% TFA followed by eluting the fluorescent material with 25 ml of methanol and 25 ml of 70% acetonitrile. Fractions were collected in 6.25 ml volumes contained in 13×100 mm borosilicate tubes and each assayed for collagen, ninhydrin-reactive nonspecific amino acids, UV at 220 and 350 nm, fluorescence at ex/em 370/440 nm as well as total salt concentration. Collagen was measured by hydroxyproline [17] and amino acids by ninhydrin [18]. Total salt concentration in each fraction was measured by precipitating the calcium salts [17] with silver nitrate and weighing the precipitate after drying (Speed-Vac, Savant/ThermoFisher).

Analytical assays for LW-1

Levels of LW-1 were assayed in skin collagen samples and its purification fractions by HPLC monitored by relative fluorescence and/or MS.

Fluorescence

LW-1 levels were assayed in enzymatic digests of insoluble skin collagen by HPLC monitoring for fluorescence at ex/em 370/440 nm. For all studies, it was assumed that collagen comprises 14% hydroxyproline wt/wt [19]. For the initial studies, digests ≈ 89.6 μg hydroxyproline (≈ 64 μg collagen) in 100 μl was injected onto a $25 \text{ cm} \times 4.6 \text{ mm}$, 5 μm Discovery BIO Wide Pore C18 HPLC column (Sigma–Aldrich) operated at flow rates 1 ml/min. However, other studies used a smaller column injecting 8.96 μg hydroxyproline onto a $15 \text{ cm} \times 2.1 \text{ mm}$ Discovery HS, C18, 3 μm HPLC column (Sigma–Aldrich) operated at flow rates 0.2 ml/min. The HPLC system was comprised by Waters Model 515 pumps, 717 autosampler, and a 680 gradient controller. Separation was by a two solvent gradient system comprised by solvent A: 98% water–2% acetonitrile containing 0.13% heptafluorobutyric acid (HFBA); and solvent B: 60% acetonitrile–40% water. Two gradient methods were used with this column as follows: (I) 0–10 min, 100% A; 10–120 min, 0–100% B (linear); (II) 0–5 min, 100% A; 5.1–100 min, 5–36% B (linear); 101–112 min, 100% B. LW-1 eluted at approximately 57 and 81 min with gradients (I) and (II), respectively. The eluate from the column was directed onto a JASCO Model 821-FP Spectrofluorometer (JASCO, Easton, MD). Chromatograms were recorded with a Dell Optiplex GX110 computer loaded with AZUR v3.0 software (Datalys, St. Martin D'Herès, France).

Mass spectrometry

Digest ≈ 8.96 μg hydroxyproline was injected in 10 μl volumes onto a $25 \text{ cm} \times 2.1 \text{ mm}$ Supelcosil LC-18-DB, 3 μm column (Sigma–Aldrich) which was ran at a flow rate of 0.15 ml/min. The HPLC system consisted of a MAGIC 2002 HPLC (Michrom BioResources, Auburn, CA) and a ALCOTT Model 719 Autosampler (ALCOTT, Norcross, GA). Separations were achieved with a two solvent gradient system consisting of solvent A: 100% water with 0.05% formic acid and 0.005% HFBA; solvent B: 60% acetonitrile–40% water with 0.05% formic acid. The following gradient was used: 0–5 min, 12% B; 5.1–20 min, 16–25% B (linear); 21–33 min, 100% B. Eluate from the column was directed onto a Finnigan LCQ-Duo MS (Thermo Electron Corporation) interfaced and controlled by a Dell Dimension 4700 computer loaded with Xcalibur v1.3 software. Selected reaction monitoring (SRM) was used to quantify LW-1 levels using d_6 -ornithine as the internal standard. In the SRM, the instrument was programmed to run in two segments over a 30 min period: segment 1, from 0–16 min, monitoring for parent ion mass at m/z 139 for d_6 -ornithine and measuring its daughter ion fragment at m/z 121 using collision energy (CE) of 22%; segment 2, from 16 to 20 min, monitoring for parent ion mass at m/z 623 for LW-1 and its daughter ion fragment at m/z 447 using CE of 32%. For some

² Deceased.

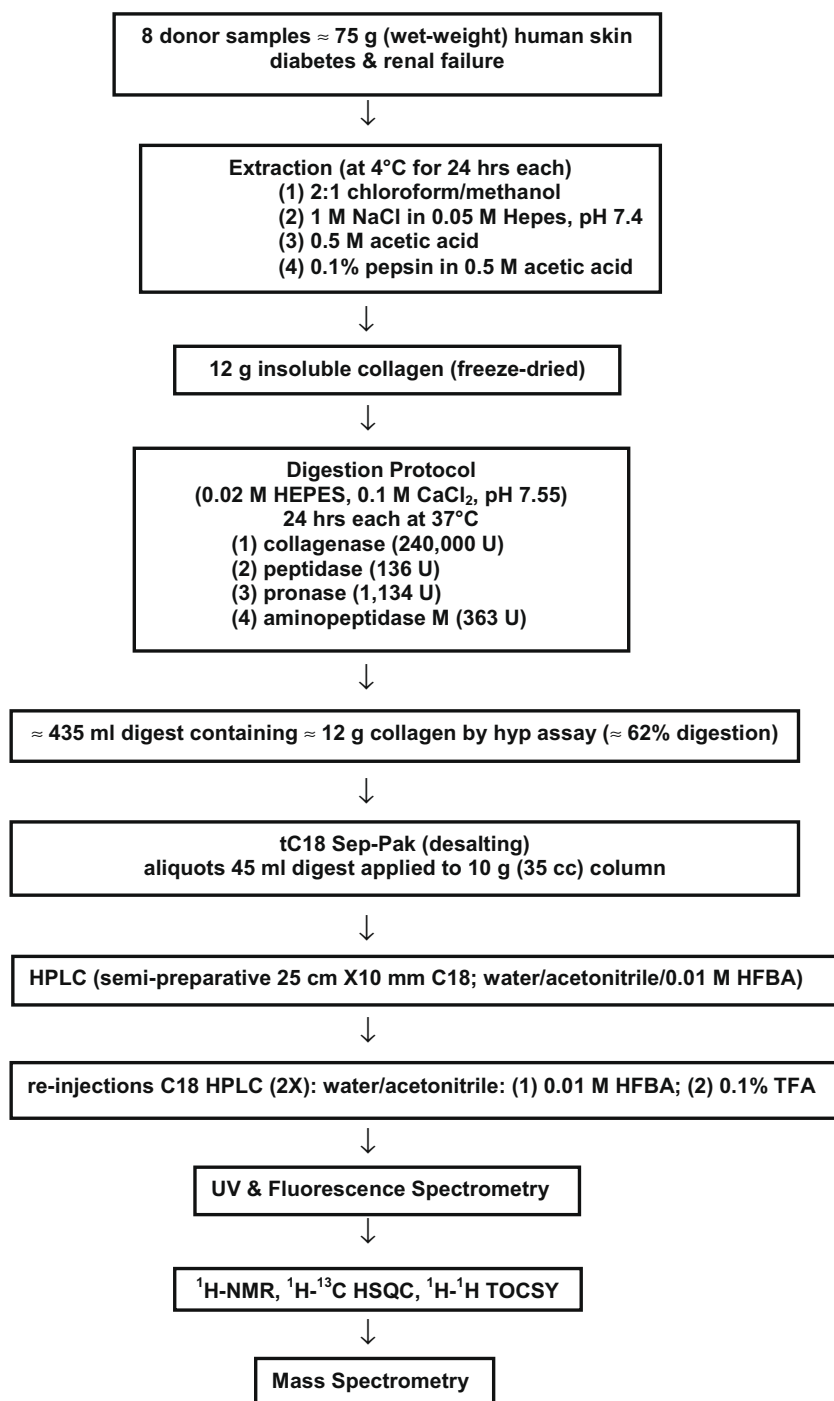


Fig. 1. Flow-chart summary of LW-1 isolation, purification, and structural analysis procedures.

runs, the HPLC was monitored by an on-line JASCO spectrofluorometer converting the analog to digital signal by a SSI SS420X converter box (Scientific Software, Lincolnwood, IL) for recording by Xcalibur.

Purification of LW-1 by HPLC

As summarized in Fig. 1, LW-1 was purified from the digest by repeated injections and collections using the aforementioned Waters HPLC system monitored by fluorescence. In these separations, digest in ≈ 2 ml volumes was injected onto a 25 cm × 10 mm, 5 μm Discovery BIO Wide Pore semi-preparative C18 column

equilibrated and eluted at a flow rate of 2 ml/min. For the first collection, the same gradient program (II) and solvent system as described in the above was used. The collected peak was freeze-dried followed by re-injection onto the same column equilibrated and eluted with the same solvents but using the following gradient: 0–5 min, 16% B; 5.1–57 min, 16–20% B (linear); 58–68 min, 100% B. The collected peak was again freeze-dried followed by a third injection using the same HPLC system but replacing HFBA by 0.1% TFA in solvent A and using the following gradient: 0–5 min, 100% A; 5.1–40 min, 1–20% B (linear), 41–53 min, 100% B. A fourth and final collection involved passing the purified LW-1 through a 25 cm × 4.6 mm, 5 μm Discovery BIO Wide Pore C18

HPLC column (Sigma–Aldrich). For this final passage, the eluate was monitored in addition to fluorescence by an on-line Waters PDA 2996 diode array UV detector. Using these four collection protocols, LW-1 eluted at approximately 74, 43, 38, and 30 min, respectively. After purification and NMR analysis, LW-1 was weighed with an analytical lab balance (Mettler AE240, Mettler-Toledo, Columbus, OH) and corrected for TFA salt assuming 2:1 TFA:LW-1 (mol/mol).

NMR procedures

Purified LW-1 was exchanged by repeated 3 × freeze-drying and reconstitution with deuterium oxide. The final preparation was reconstituted with 350 µl deuterium oxide followed by filtering through a Cameo 3A 0.45 µm syringe-type filter (ThermoFisher). The sample was placed in a 180 × 4.2 mm Shigemi NMR tube and sealed with a glass plunger (BMS-005B, Shigemi, Allison Park, PA). For ^1H NMR, the sample was scanned for 24 h with a Bruker 800 MHz NMR spectrometer (Bruker BioSpin Corporation, Billerica, MA) equipped with a cryoprobe (Cleveland Center for Structural Biology, Cleveland, OH). For ^1H – ^1H TOCSY (total correlation spectroscopy) and ^1H – ^{13}C HSQC (heteronuclear single quantum coherence) experiments, the sample was scanned for approximately 68 h each.

Mass spectrometry procedures

The molecular mass (M^+) and product ions for LW-1 were initially determined using a LCQ-Duo MS coupled to the MAGIC 2002 HPLC system described in the above. This employed using the full mass and MS/MS automated scanning functions of Xcalibur. The designated mass ions were subsequently reconfirmed using a Micromass Quattro Ultima MS API detector (Waters). For this setup, a 5 µl aliquot diluted sample of LW-1 was injected onto a 2.1 × 50 mm Atlantis dC18, 3 µm column (Waters) using a Alliance 2695 HPLC system (Waters). The mobile phase consisted of 80% water–20% acetonitrile containing 0.1% formic acid buffered to pH 3.6 with ammonia which was run isocratically through the column at flow rate 0.2 ml/min. LW-1 eluted at 1.1 min with parent ion mass at m/z 623.

Both the LCQ and Ultima MS detectors were tuned with pentosidine by direct infusion. The CEs for LW-1 using the LCQ has previously been stated in the above. For the Ultima, a CE of 25 eV at cone voltage 60 V was initially applied as found optimal for the fragmentation of pentosidine. However, this CE proved inadequate to fragment LW-1 which required a CE of 35 eV with the Ultima. For computations of relative abundance for each daughter ion of LW-1 shown in Fig. 10, peak area at 1.1 min for each specific mass ion was obtained by the integration function using MassLynx software version 4.1. A total integration number was obtained by summing the areas for all positive specific scanned signals at 1.1 min and expressing each one as a percentage of the total (Fig. 10).

High resolution mass analysis of LW-1 was conducted at the Research Technology Support Facility (RTSF) for Mass Spectrometry at Michigan State University (East Lansing, MI) under the direction of Dr. A. Daniel Jones using a Micromass Q-ToF Ultima API (Waters) instrument with electrospray ionization and lock spray correction for mass drift. From this analysis, a list of possible elemental compositions was made assuming LW-1 is composed by C, H, N, O.

UV and fluorescence spectrometry

UV spectrums at different pH were obtained by a HP 8452A Diode Array Spectrophotometer. The fluorescence spectra were ob-

tained by the aforementioned JASCO Spectrofluorometer as adapted with a cuvette holder and using the AZUR chromatography software to record the spectra.

Statistics

Statistical analysis were done using procedures previously described by us [17] using either SPSS software (Graduate Pack version 16, SPSS, Inc., Chicago, IL) or statistical functions embedded in SigmaPlot software (version 11.0, Systat Software, Inc., Chicago, IL). LW-1 levels in skin collagen digests for donors listed in Supplement Table S2 were transformed using the square root transformation prior to regression analysis. These data including the regression line and 95% confidence intervals of prediction are presented in the untransformed form (Fig. 11).

Results

Preliminary investigation of LW fluorescence in human skin collagen digests

Analysis of enzymatic digests from human insoluble skin collagen revealed a single major fluorescent peak at ex/em 370/440 nm which eluted at 57.3 min by reverse phase HPLC using a very shallow gradient of acetonitrile (Fig. 2). The size of the peak; i.e., integrated relative fluorescent peak area, increased with age, but more profoundly by diabetes (Fig. 2). In further study, peak area expressed as fluorescent units/µg collagen was found greater for diabetic vs. nondiabetic donors of similar chronological age: 11 years (0.27 vs. 0.07), 28 years (0.28 vs. 0.15), and 62 years (1.66 vs. 0.23). Review of medical histories for the 47-year-old patient with type 1 diabetes (Fig. 2) and the 62-year-old patient with type 2 diabetes revealed that both had ESRD. Subsequently, the newly identified peak was named LW-1.

Properties of LW-1: reducibility by borohydride and stability to acid hydrolysis

As determined by HPLC, LW-1 was found *nonreducible* upon treatment with sodium borohydride and *not stable* to conditions of acid hydrolysis; i.e., 6 N HCl at 110 °C for 18 h (data not shown).

Comparison of HPLC RT of LW-1 with other published fluorophores

In a series of separate HPLC experiments described in the methods, LW-1 (retention time = 72 min) was found *not* to co-elute with a variety of other known fluorescent amino acids and cross-links including ST29 (39 min) [20], argpyrimidine (61 min) [21], K2P (62 min) [22], pentosidine (68 min) [23], and ONE-pyrrole (97 min) [24,25] (data not shown). The LW-1 peak was completely absent from chromatograms at the lower wavelengths used to monitor argpyrimidine (ex/em 335/385 nm), pentosidine (335/385 nm), and ST29 (284/400 nm).

Purification of LW-1

Insoluble skin collagen totaling ≈12 g after extraction and freeze-drying was sequentially digested with a series of enzymes listed in Fig. 1. As determined by hydroxyproline analysis, ≈62% of the collagen had been digested using this protocol (Fig. 1). The digest was subsequently desalted on a Sep-Pak column. As shown in Fig. 3, the calcium salts plus the bulk of the collagenous material eluted in the early fractions followed later by the elution of the highly fluorescent material which also showed strong UV absorbance at 350 nm, but considerably less collagen (Fig. 3). After col-

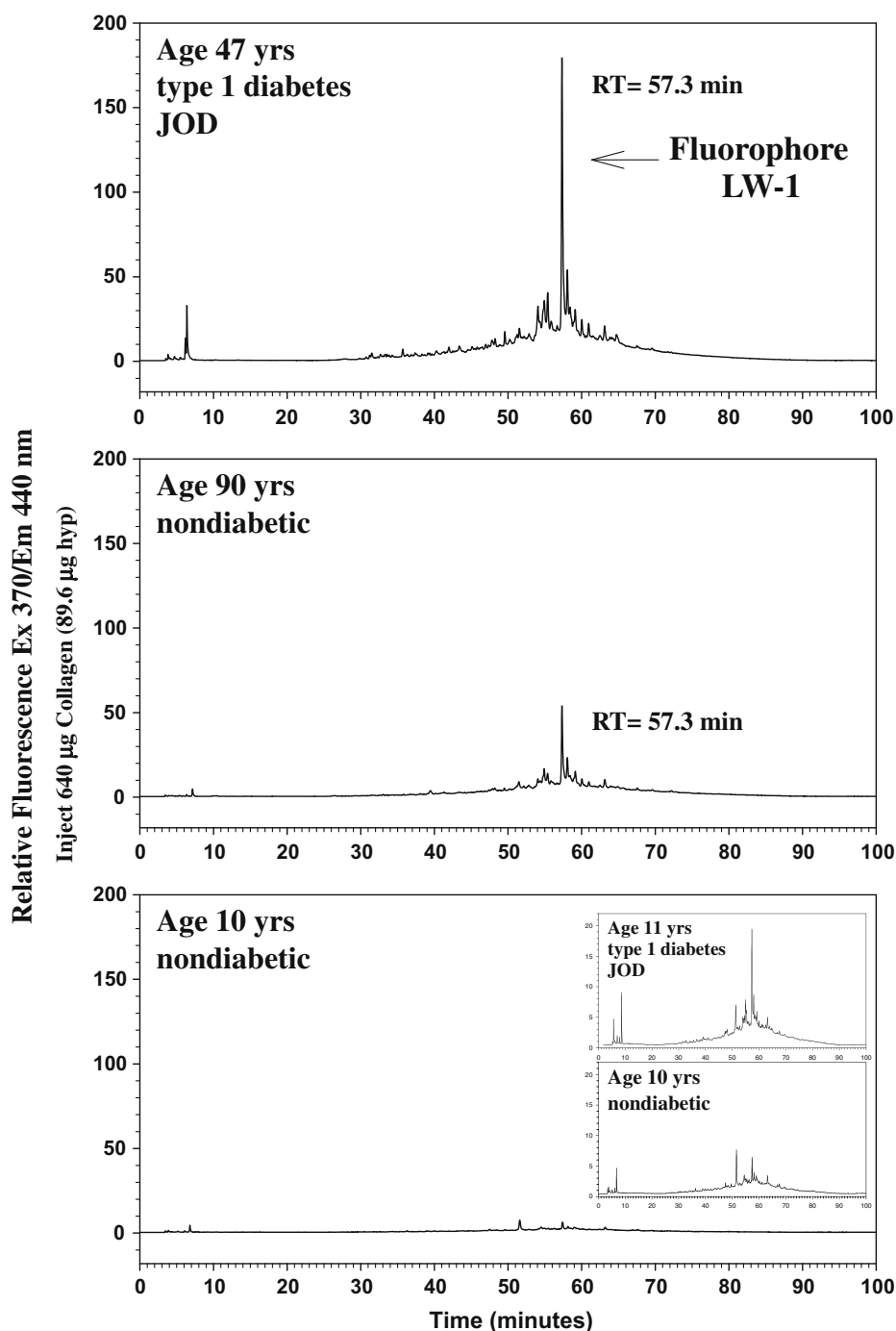


Fig. 2. HPLC chromatograms of enzymatic digests of human insoluble skin collagen from nondiabetic and diabetic donors of different ages. Collagen digest $\approx 89.6 \mu\text{g}$ hydroxyproline ($\approx 640 \mu\text{g}$ collagen) in $100 \mu\text{l}$ was injected onto a $25 \text{ cm} \times 4.6 \text{ mm}$, $5 \mu\text{m}$ Discovery BIO Wide Pore C18 column operated at flow rates of 1 ml/min using a Waters HPLC (see Materials and methods).

lecting and freeze-drying the fluorescent peak, a small aliquot was injected onto a HPLC which showed a profile according to Fig. 4. The LW-1 peak showed UV absorbance at 350 and 220 nm (not shown), ninhydrin reactivity, but no hydroxyproline (Fig. 4). After isolation of the peak by repeated injections onto the HPLC according to Fig. 1, the collected LW peak was freeze-dried and subjected to spectral analyses. Injection of a diluted aliquot of the purified LW-1 onto HPLC gave a single peak of same retention time as LW-1 assayed directly from an enzymatic digest of human insoluble skin collagen confirming that LW-1 was not altered by purification (data not shown). Purity was judged by subsequent UV,

fluorescence, NMR, and mass spectroscopy. The total yield of LW-1 was $\approx 438 \mu\text{g}$ (see Materials and methods).

UV and fluorescence spectroscopy of LW-1: the effect of pH on maxima

LW-1 had a UV maximum (UV_{max}) at 348 nm and excitation/emission ($\text{ex}_{\text{max}}/\text{em}_{\text{max}}$) fluorescence maxima at 348/465 nm (em_{max} range $\approx 440\text{--}470 \text{ nm}$), respectively (Fig. 5). There were no bathochromic shifts in these maxima when the pH was varied from 2 to 12 (Fig. 5). However, the amplitude of the ex_{max} and em_{max} varied reaching a maximum and minimum at pH 7 and 12, respectively (Fig. 5).

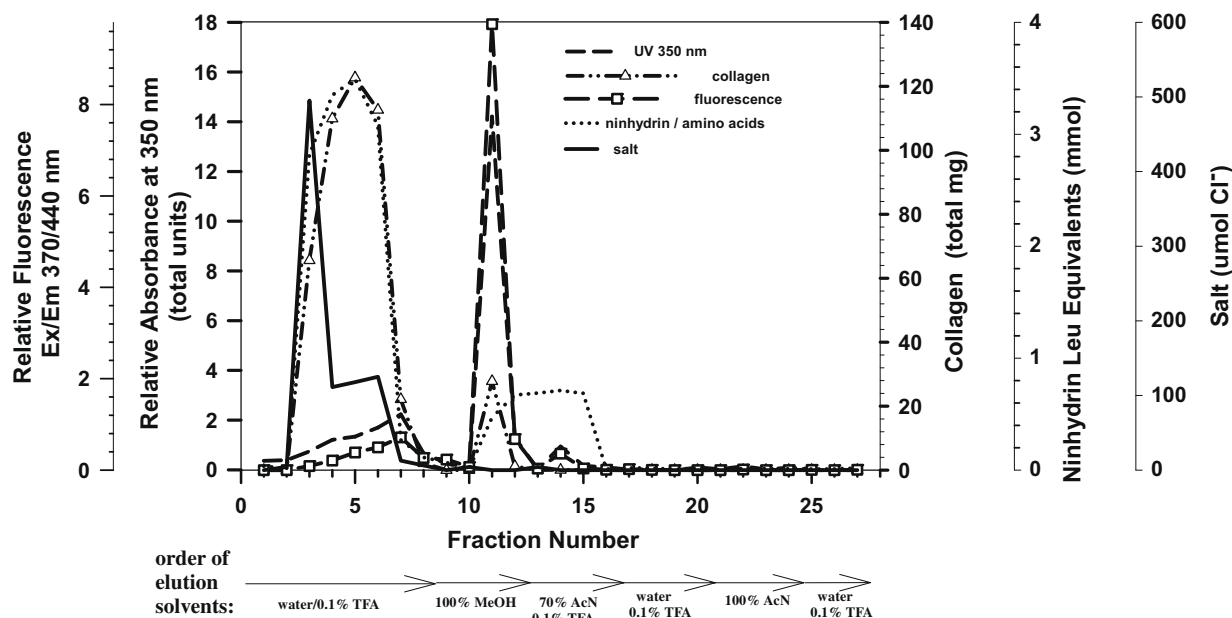


Fig. 3. Chromatogram showing desalting and concentration of enzymatic digest from skin digest on a Waters Sep-Pak tC₁₈ 10 g column. Approximately 650 mg collagen in ≈25 ml volume was applied to a 10 g Waters Sep-Pak tC₁₈ column. Fractions of approximate 6.25 ml volumes were collected and each was assayed for UV (350 nm), fluorescence (ex 370/em 440 nm), collagen (hydroxyproline after acid hydrolysis), total amino acids (ninhydrin), and total salt (silver nitrate precipitate).

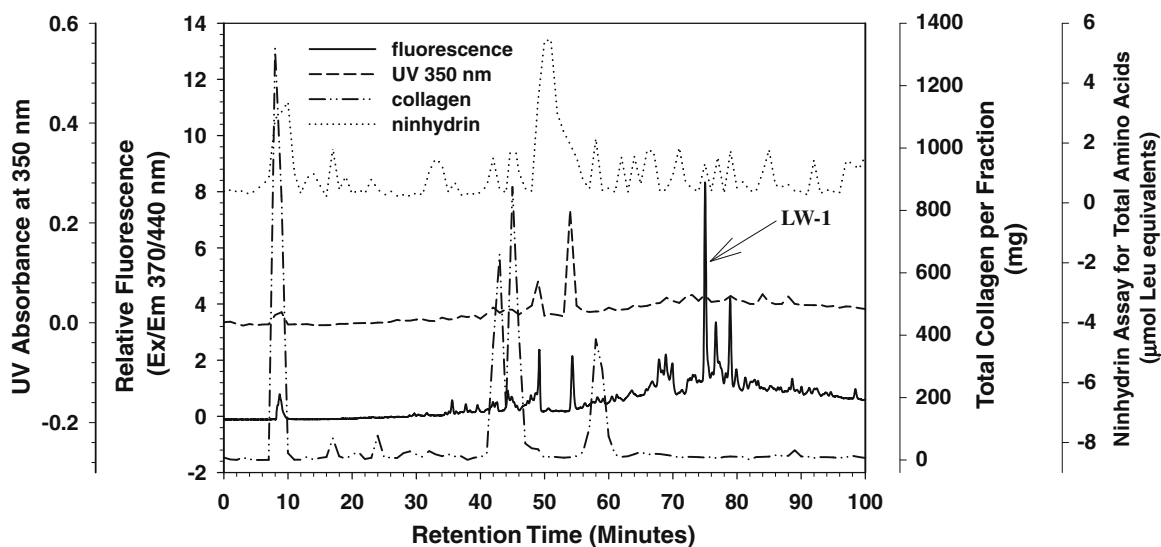


Fig. 4. Representative HPLC chromatogram profile of the LW fluorescent fraction collected from the desalting column (see Fig. 3). The highly fluorescent material collected from one run of the desalting column (representing ≈25 ml original digest) was freeze-dried and reconstituted to 2.2 ml with HPLC solvent A. A total of 400 μl of this material was injected onto a 25 cm × 10 mm, 5 μm Discovery BIO Wide Pore C18 column ran at flow rate 2 ml/min of which 2 ml fractions were collected. Fluorescence was measured at ex/em 370/440 nm; collagen by hydroxyproline; amino acids by ninhydrin.

NMR of LW-1: interpretation of ¹H NMR, ¹H–¹³C HSQC, and ¹H–¹H TOCSY

As shown in Fig. 6, the ¹H NMR spectrum revealed that LW-1 had three signals *a*, *b*, *c* in the far downfield region at 8.65 (singlet), 8.02 (doublet, *J* 3.2 Hz), and 6.95 (doublet, *J* 3.2 Hz) ppm with integral ratio of 1:1:1, respectively. A ¹H–¹³C HSQC experiment showed that each of these protons was bound to carbon atoms with chemical shifts at 110, 138, and 96 ppm, respectively (Table 1 and Fig. 7, upper plot). These results for both the ¹H and ¹³C chemical shifts suggest that signals *a*, *b*, *c* represent the aromatic region of LW-1. In addition, a ¹H–¹H TOCSY experiment showed strong coupling between protons *b* and *c* (signals *bc* and *cb*, Fig. 8) due

to vicinal coupling and weak cross-signals between protons *a* and *c* as a result of long-range (*1r*) coupling; i.e., signals *ac*^{*1r*} and *ca*^{*1r*}, Fig. 8. The same experiment showed that none of these protons correlated with protons in the aliphatic region either by short- or long-range coupling (data not shown) probably because TOCSY transfer was disrupted by the presence of a heteroatom. By comparison with published data on chemical shifts and coupling constants for vesperlysines [26], these results suggests that protons *b* and *c* are part of a heteroaromatic five-member ring structure with the heteroatom most likely being nitrogen where proton *b* is closer to the heteroatom. Furthermore, the chemical shifts and moreover the coupling constants between protons *b* and *c* suggests the presence of an additional condensed six-member (hetero)-aro-

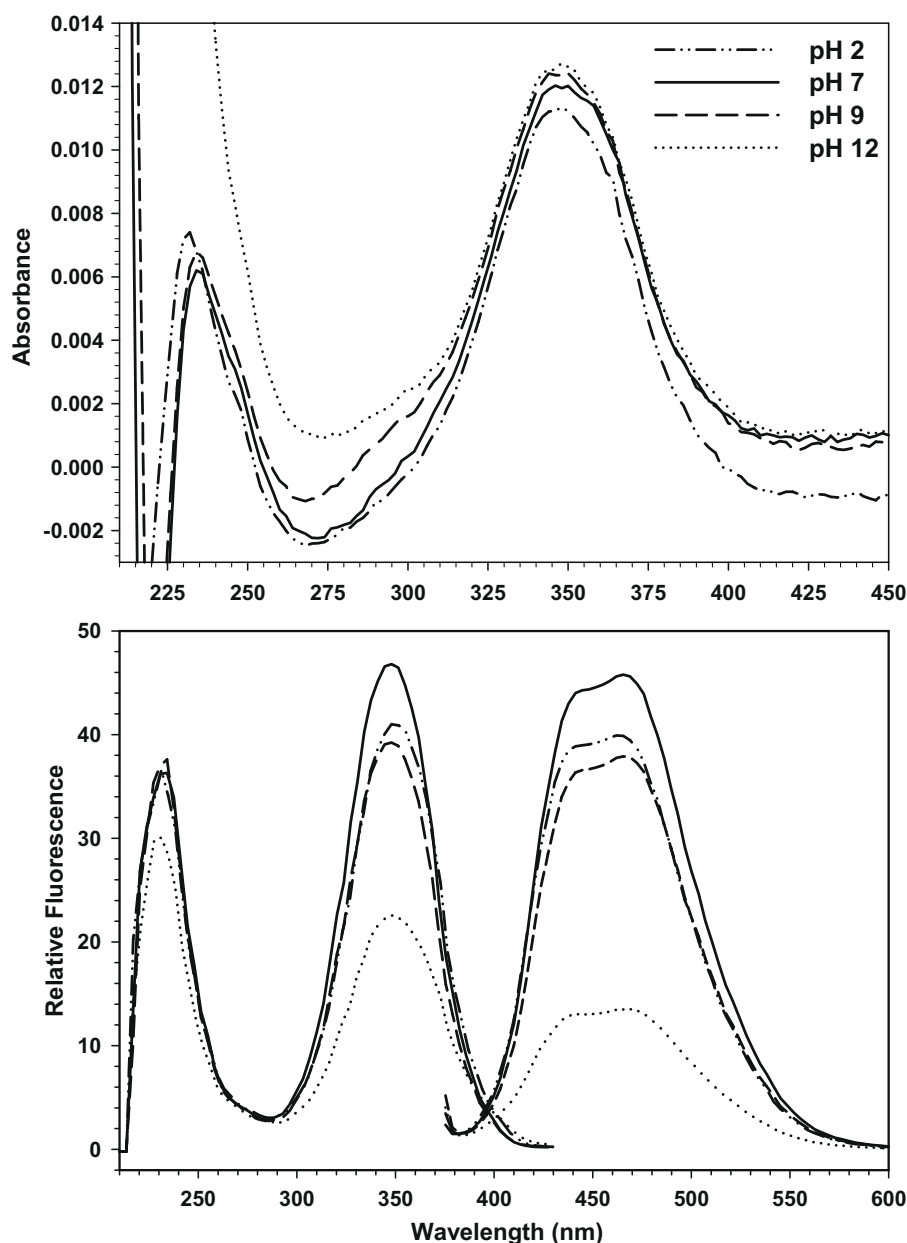


Fig. 5. The effects of pH on absorbance and fluorescent spectra of LW-1 in 0.1 M sodium phosphate buffer.

matic ring of which proton *a* is a member and in proximity to proton *c* of the adjacent ring.

The most prominent signal in the ^1H spectrum is at 2.69 ppm (labeled as proton signal *d* in Figs. 6–8) which integrated to three protons (data not shown). These protons correlated to a single carbon atom at 13 ppm (Fig. 7) which suggests the presence of a methyl group attached to a six-member aromatic ring. In support, there are similarities in the ^1H and ^{13}C chemical shifts at 2.69 and 13 ppm for the methyl group of LW-1 (Table 1) compared to that reported for the aromatic methyl group of vesperlysine B; i.e., 2.8 and 15.4 ppm, respectively [26].

Signal *e* at 3.70 ppm (Fig. 6) bound on a carbon atom with chemical shift of 55 ppm (Table 1 and Fig. 7) corresponds to the α -proton of an amino acid. The TOCSY spectrum (Fig. 8) showed cross-signals between protons *e* and protons labeled as *g*, *h*, and *i* at 2.0, 1.88, and 1.35 ppm, respectively. The same experiment showed also correlation between signals *g*, *h*, and *i* with signal *f* at 4.43 ppm (Fig. 8) bound on a carbon atom at 47 ppm (Fig. 7) sug-

gesting amino acid lysine as a part of the LW-1 structure. Since triplet *f* shares chemical shifts with equivalent protons in pentosidine [23] as well as many other proteinaceous cross-links [26–31], this signal was attributed to the ϵ -CH₂ (methylene) group of a lysine residue incorporated into an aromatic ring through its ϵ -amino group. Interestingly, the ^1H , ^{13}C chemical shifts and the coupling constant reported here for this triplet signal *f* of LW-1 (4.43 ppm, 47 ppm, 7.0 Hz) are equivalent to those reported for the ϵ -CH₂ group of vesperlysine B bound on a pyridinium ring (4.32, 48.9, 7.0 Hz) [26]. Although similarity with vesperlysine B suggests ϵ -amino group of LW-1 lysine as a part of a pyridinium ring, at this moment there is no unequivocal data which proves lysine as a part of a pyridinium (6 member) or pyranium (5 member) aromatic ring. Signals *g*, *h*, and *i* were assigned as β -, δ -, and γ -methylene groups of lysine, respectively.

Multiple signals *j_a* and *j_b* at 5.30 and 4.96 ppm, respectively, integrating as 1 proton each (Fig. 6) are bound on the same carbon atom at 52 ppm (Table 1 and Fig. 7). The TOCSY experiment showed

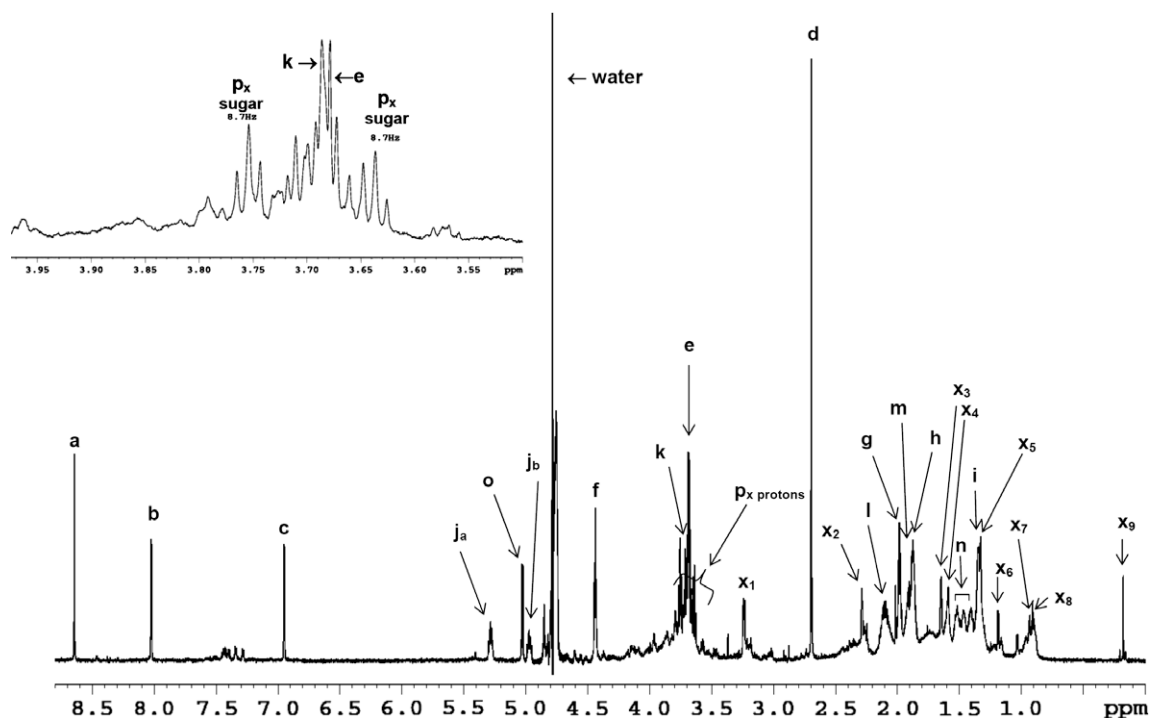


Fig. 6. Proton NMR spectrum of LW-1 determined by an 800 MHz Bruker NMR instrument. Insert: magnification of region 3.5–4 ppm.

Table 1

Summary of signal assignments for the ^1H NMR, ^1H – ^{13}C HSQC, and ^1H – ^1H TOCSY spectra determined for LW-1^a.

Label position Figs. 6–8 signal ID	δ ^1H chemical shifts (ppm)	Signal splitting ^b (J, Hz)	δ ^{13}C chemical shift from HSQC (ppm)	^1H – ^1H TOCSY correlations signal ID	Structural assignment
a	8.65	s	110	c	Six-member aromatic ring
b	8.02	d (3.2)	138	c	Five-member aromatic ring
c	6.95	d (3.2)	96	b, a	Five-member aromatic ring
d	2.69	s	13	None	–CH ₃ on six-member aromatic ring
e	3.70	t overlap	55	g, h, i	α -CH of lysine
f	4.43	t (7.0)	47	g, h, i	ϵ -CH ₂ of lysine
g	2.00	m	29	e, f, h, i	β -CH ₂ of lysine
h	1.88	m overlap	31	e, f, g, i	δ -CH ₂ of lysine
i	1.35	m overlap	24	e, f, g, h	γ -CH ₂ of lysine
ja	5.30	m	52	j _b , l, m, n	Unknown
jb	4.96	m	52	ja, l, m, n	Unknown
k	3.72	m overlap	?55 or 63	l, m, n	Unknown
l	2.10	m overlap	28	ja, jb, k, m, n	Unknown
m	1.92	m overlap	30	ja, jb, k, l, n	Unknown
n	1.50	m overlap	22	ja, jb, k, l, m	Unknown
o	5.05	d (7.8)	?(>80)	p _{protons}	CH ₁ sugar moiety?
p _{protons}	3.60–3.85	m overlap	70, 72, 73, 75, 77	o	CH _n sugar moiety
x ₁	3.24	t	38	x ₄ , x ₅	Unknown
x ₂	2.28	s	36	x ₃	Unknown
x ₃	1.64	s	27	x ₂	Unknown
x ₄	1.59	s?	25.5	x ₁ , x ₅	Unknown
x ₅	1.33	s? overlap	20	x ₁ , x ₄	Unknown
x ₆	1.19	d	?	None	Unknown
x ₇	0.93	d	?	None	Unknown
x ₈	0.9	t	?	None	Unknown
x ₉	0.17	s	?	None	Unknown

^a ?, tentative.

^b s, singlet; d, doublet; m, multiplet.

germinal coupling between these two protons as well as cross-signals between j_a and j_b with l , m , and n protons. Proton k also showed cross-signals with the same protons (l , m , n) in the TOCSY spectrum (Fig. 8). Although the ^1H chemical shift for signal k corresponded to ^1H chemical shifts characteristic for α -CH of amino acids, it cannot be unequivocally assigned as evidence for an addi-

tional amino acid because of its overlap with proton signals e and p (Fig. 6) as well as its non-clearly-defined signal in the HSQC spectrum (Fig. 7).

Signal o at 5.05 ppm is a doublet (J 7.8 Hz) integrating to 1 proton (Fig. 6 and Table 1). It did not show any cross-signals in the HSQC spectrum (Fig. 7). However, it was assumed that its carbon

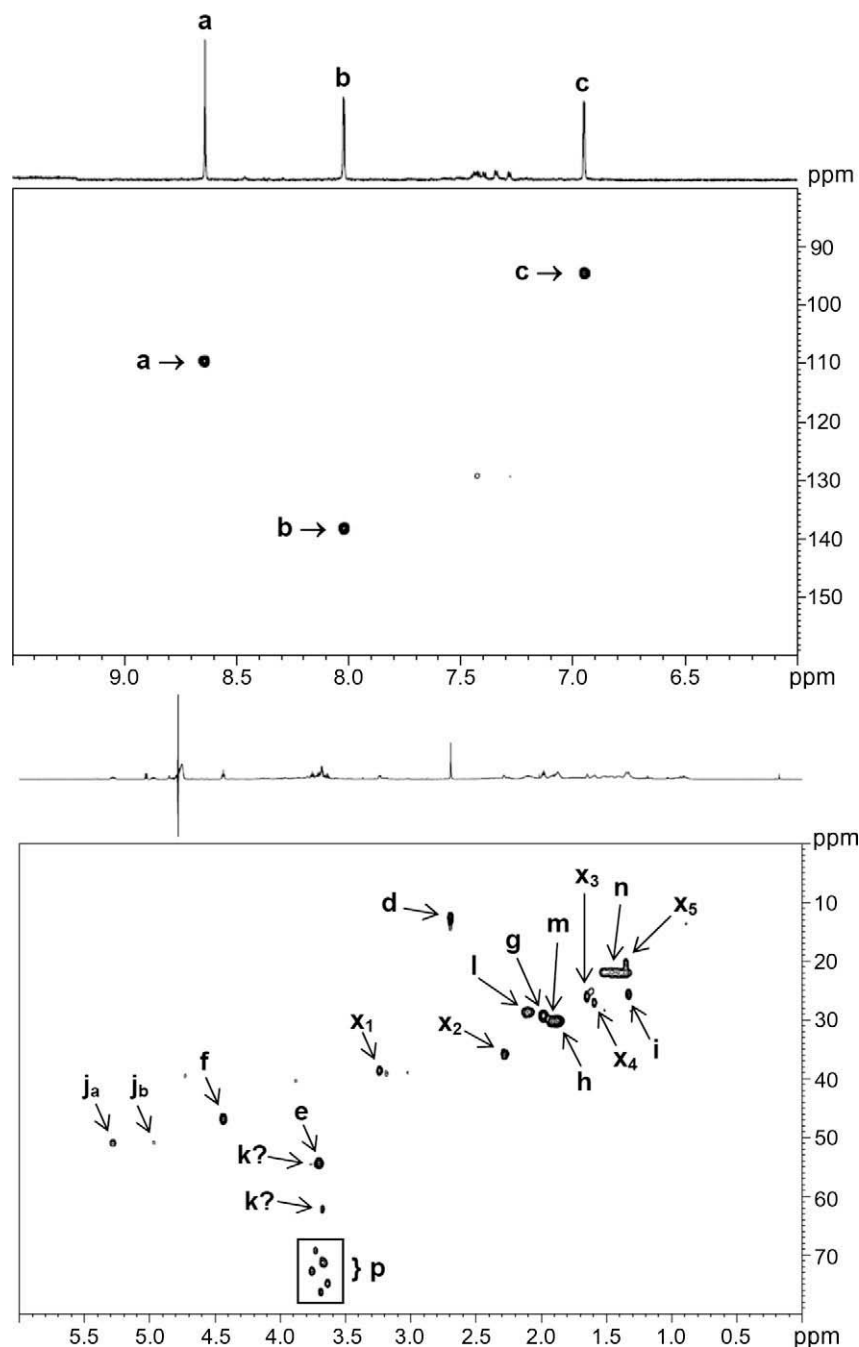


Fig. 7. ^1H – ^{13}C heteronuclear single quantum coherence (HSQC) NMR spectrum for LW-1. The HSQC was constructed in two separate experiments: aromatic (upper plot) and aliphatic region (lower plot).

atom had a signal >80 ppm which could not be determined in the HSQC due to data collections were done separately for the aliphatic and aromatic regions (Fig. 7). Signal *o* showed correlation with protons labeled as *p* protons (Fig. 8). A similar signal with the same type of split and chemical shift was noted in the high resolution NMR spectroscopic metabolic investigations of rat liver by Bollard et al. [32] with reported ^1H and ^{13}C chemical shifts of 5.24 and 92.7 ppm, respectively, which was assigned to the C_1H group of α -glucose [32]. In addition, ^1H (3.60–3.85 ppm) and ^{13}C (70–77 ppm) chemical shifts of the *p* signals (Figs. 6 and 7) correspond to chemical shifts characteristic for sugars [32]. However, because of their signal complexity and overlap, as well as the lack of spec-

tra; i.e., a ^{13}C NMR and a continuous HSQC (Fig. 7), it was not possible to determine individual assignment based upon these results.

As shown in the ^1H NMR spectrum of Fig. 6, additional signals labeled x_n were observed where $n = 1$ –9 (Table 1). Proton signal x_1 at 3.24 ppm coupled to a carbon at 38 ppm (Fig. 7) and correlated with proton signals x_4 and x_5 at 1.59 and 1.33 ppm (Fig. 8). Likewise, proton signal x_2 at 2.28 ppm coupled to a carbon atom at 36 ppm (Fig. 7), but correlated only with proton signal x_3 at 1.64 ppm (Fig. 8). Finally, proton signals x_6 – x_9 at 1.19–0.17 ppm showed neither carbon coupling nor proton correlations (Figs. 7, 8 and Table 1). Collectively, these signals can be the part of the LW-1 structure or impurities present in the sample.

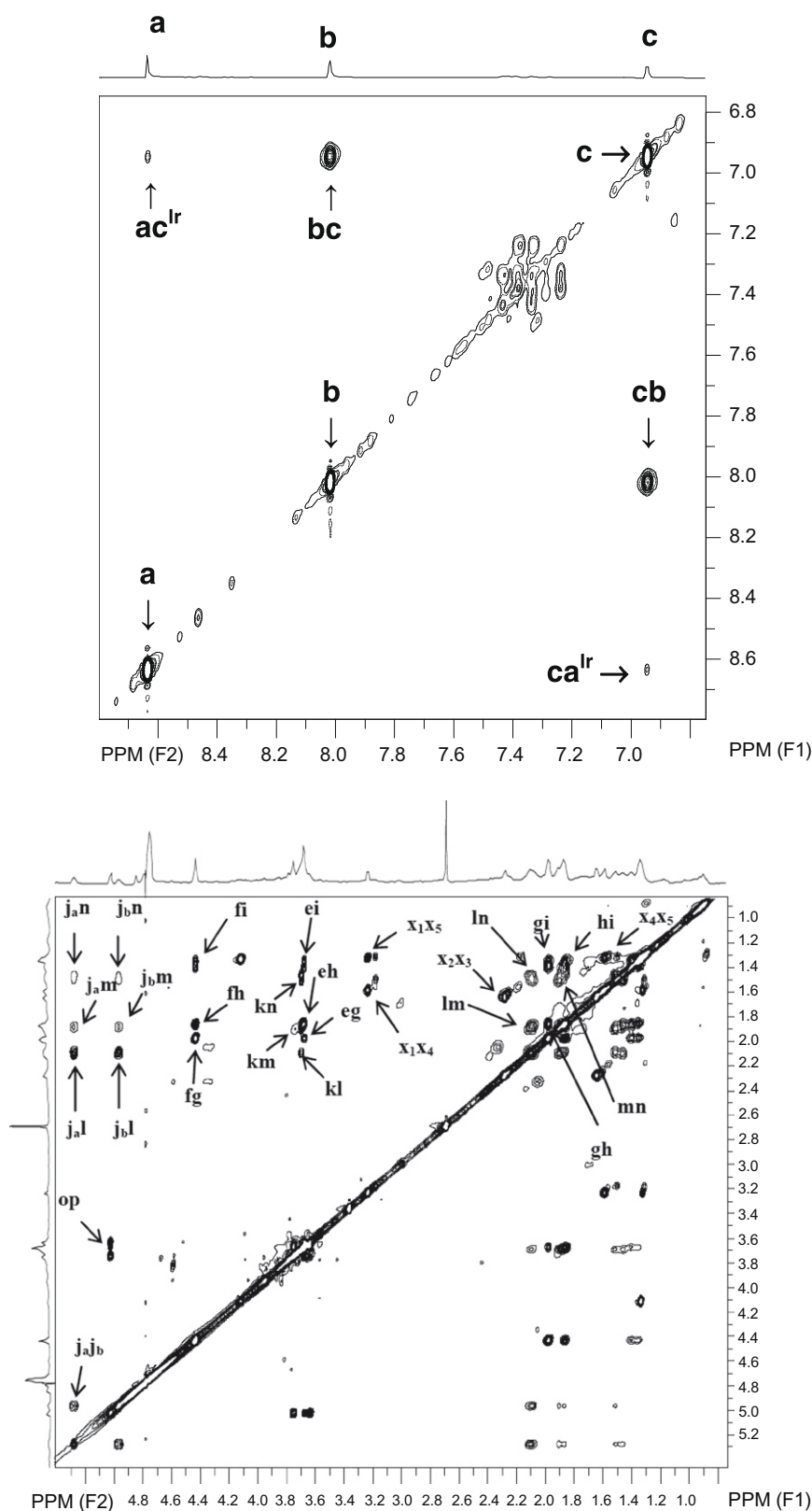


Fig. 8. ^1H – ^1H total correlated spectroscopy (TOCSY) NMR spectrum for LW-1: aromatic (upper plot) and aliphatic region (lower plot). lr: long-range.

Mass analysis of LW-1

LW-1 eluted as a single fluorescent peak at 19.2 min with a parent ion at m/z 623 when monitored by an ion-trap MS (LCQ-Duo,

Fig. 9). An additional minor signal at m/z 312 was also observed in the full MS (Fig. 9). MS/MS analysis showed daughter ions at m/z 447 > 318 > 494 (data not shown). These signals were subsequently confirmed with a triple quadrupole MS (Micromass

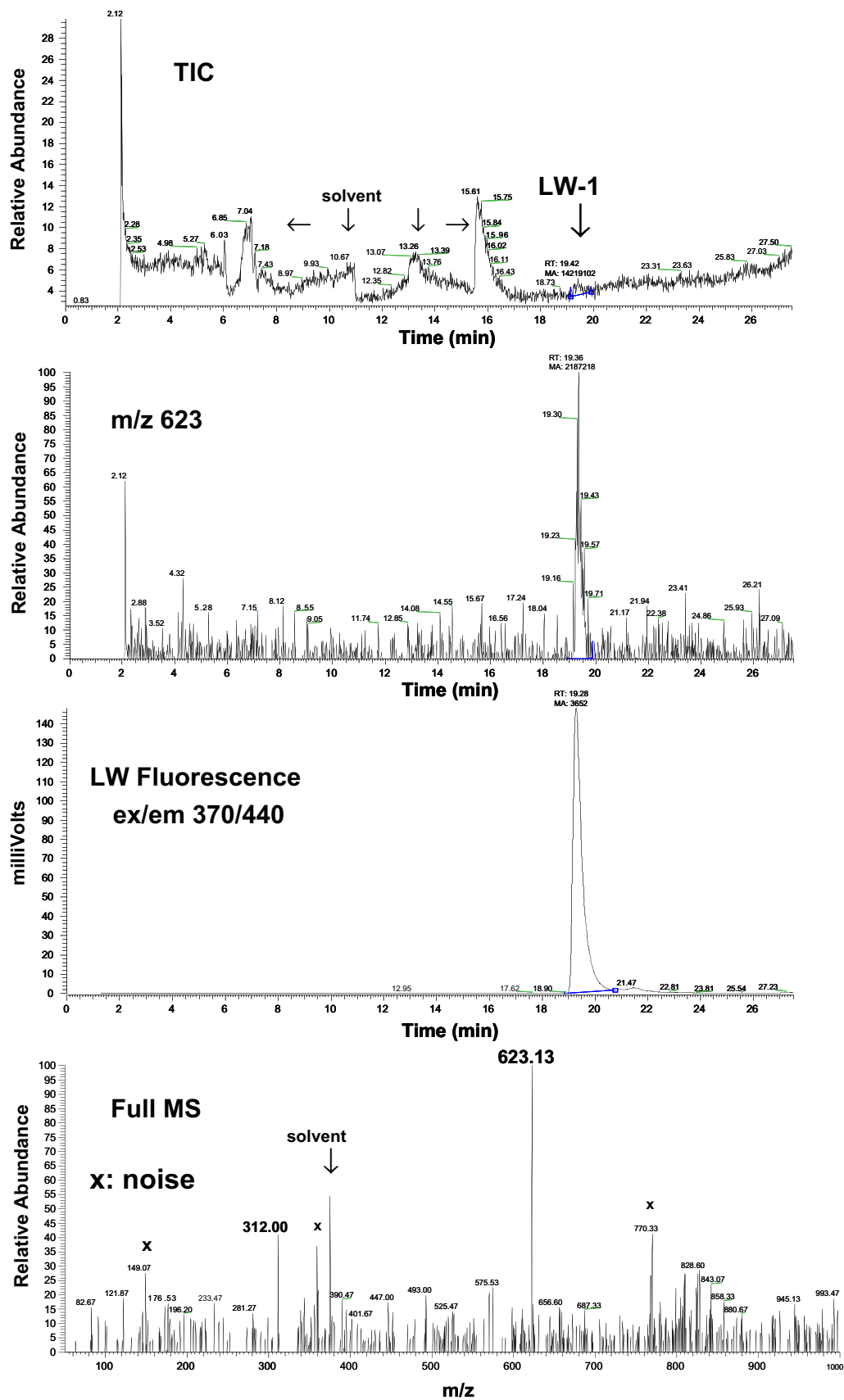


Fig. 9. LW-1 eluted at 19.4 min using HPLC monitored by MS (LCQ-Duo) and fluorescence detection. (A) TIC: total ion current MS; (B) reprocessed chromatogram at m/z 623; (C) fluorescent chromatogram; and (D) full MS spectrum of LW-1.

Quattro Ultima) with additional signals noted at m/z 130, 177, 263, 273, 386, 402, 430, 578 (Fig. 10). By far the largest signal was at m/z 447 (Fig. 10).

Chemical assignments of observed fragments from the MS/MS spectrum

Fragments at m/z 578 corresponds to $M^+ - \text{COOH}$; 494, $M^+ - \text{norleucine}$ \approx loss of a deaminated lysine residue explained by the signal at m/z 130 (Fig. 10), also observed in the MS/MS spectrum of pentosidine [23] and vesperlysine A [31]; 447, loss of a 176 fragment possibly representing the sugar portion of the LW-1 molecule as previously discussed for NMR data (Figs. 7 and 8); 318, the loss of (176 + norleucine); 402, loss of (176 + COOH); 273, loss of (176 + COOH + norleucine); 386, loss of (176 + COOH + NH_2); 430, loss of (176 + OH).

Exact mass determination and possible empirical formulas

The exact mass of LW-1 was determined to be 623.2746 ± 0.0017 by a Micromass Q-ToF Ultima API MS (RTSF-Mass Spectrometry Facility, Michigan State University, East Lansing, MI). Possible empirical formulas for LW-1 with an elemental composition composed by C, H, N, O are shown in Table 2. Evaluation of the C24 formula shows that it can be ruled out because of no nitrogen. Other excluded formulas include those with an unlikely high number of nitrogen atoms; i.e., N10 to $\text{N}20 \approx \text{C}16$, C17, C18, C21, C22, C23 can also be excluded. Thus, the elemental composi-

tion of LW-1 can be narrowed down to candidate formulas with C20, C25, and C26 composed by N6, N4, and N8, respectively (Table 2).

LW-1 levels in insoluble human skin collagen determined by HPLC/SRM-MS

Levels of LW-1 were determined in insoluble collagen samples from human skin obtained at autopsy. For this assay, a HPLC on-line to the LCQ-Duo MS instrument was used (Fig. 9) employing a SRM method; i.e., m/z 623 \rightarrow 447. Skin samples used in this assay including a list of major diagnoses at death for each patient are summarized in the supplement (Table S2). The results showed that LW-1 fluorescence strongly correlated with SRM signal m/z 447 ($r = 0.94$, $n = 14$, $P < 0.0001$, data not shown). LW-1 levels significantly ($P < 0.0001$) increased with age at an exponential rate in nondiabetic subjects as modeled by a quadratic function ($r = 0.92$, $n = 13$, $P < 0.0001$, Fig. 11). Levels were also significantly elevated by chronic and ESRD ($P = 0.021$) as well as diabetes ($P < 0.0001$, Fig. 11). Most notable, there were $n = 5$ outliers for nondiabetic patients; i.e., levels elevated above the 95% confidence interval for the regression line determined for nondiabetics (Fig. 11). Examination of their medical histories including postmortem records showed that they all died with chronic and severe respiratory problems including pulmonary hemorrhage, edema, emphysema, and severe alveolar damage (Supplement Table S2). However, many other

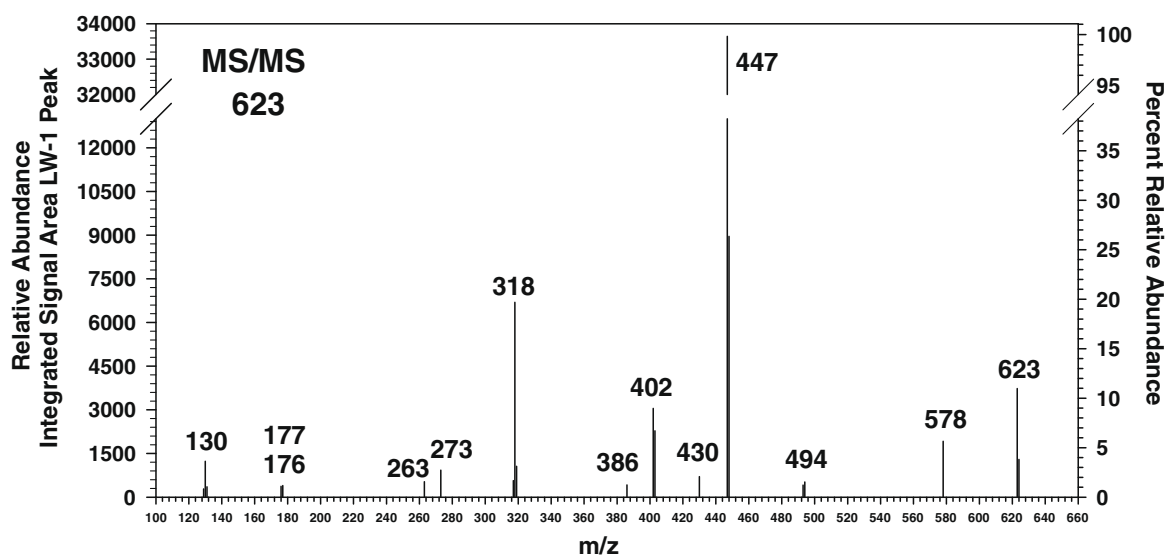


Fig. 10. Fragmentation pattern (MS/MS) of LW-1 using a Waters Quattro Ultima mass spectrometer. Purified LW-1 was injected onto a 2.1×50 mm Waters Atlantis dC18, $3 \mu\text{m}$ column ran under isocratic conditions at a flow rate 0.2 ml/min. Peak area for LW-1 which eluted at 1.1 min was determined for each signal and expressed as a percentage of the total as shown.

Table 2

Predictive elemental composition of LW-1 based upon C, H, N, O.

Calculated mass LW-1 (Da)	Difference from exact mass (623.2746 ± 0.0017) (mDa)	Number of nitrogen atoms (n)	Predicted empirical formula
623.2762	−1.6	0	C24 H47 O18
623.2776	−3.0	4	C25 H43 N4 O14
623.2736	1.0	6	C20 H43 N6 O16
623.2789	−4.3	8	C26 H39 N8 O10
623.2749	−0.3	10	C21 H39 N10 O12
623.2709	3.7	12	C16 H39 N12 O14
623.2762	−1.6	14	C22 H35 N14 O8
623.2722	2.4	16	C17 H35 N16 O10
623.2776	−3.0	18	C23 H31 N18 O4
623.2735	1.1	20	C18 H31 N20 O6

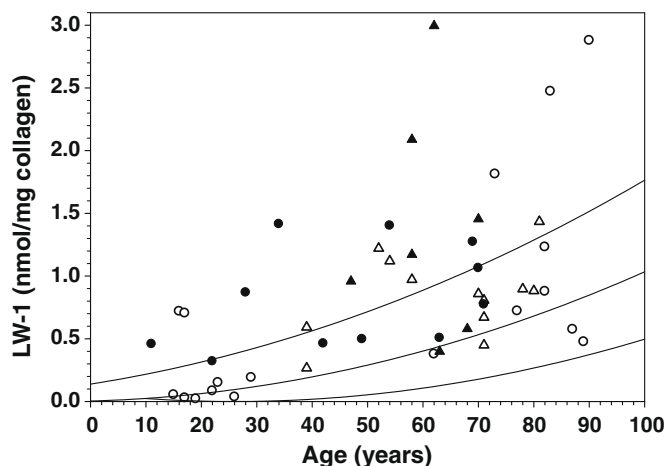


Fig. 11. Selective reaction monitoring (SRM) of LW-1 levels in enzymatic digests of human insoluble skin collagen as a function of age, diabetes, and renal failure. Parent ion at m/z 623 was selected and monitored for product (daughter) ion at m/z 447. The enclosed lines represent the regression line and 95% confidence intervals of prediction determined for LW-1 levels of nondiabetic individuals without renal failure. CRF: chronic renal failure; ESRD: end-stage renal disease. Regression line equation: $9 \times 10^{-5}x^2 + 1.2 \times 10^{-3}x + 3.7 \times 10^{-3}$, $n = 13$, $r = 0.92$, $P < 0.0001$. \circ , nondiabetic; \triangle , nondiabetic w/CRF or ESRD; \bullet , diabetic; \blacktriangle , diabetic w/CRF or ESRD.

nondiabetic patients with levels within the confidence interval of Fig. 11 were also diagnosed at death with respiratory problems as well, although more acutely and with less severity.

Discussion

In spite of our successful isolation and purification of LW-1, the above instrumental analyses have revealed a surprisingly large molecule and a complex structure that unfortunately could not be synthesized using traditional Maillard reaction chemistry as we have done in the past for pentosidine and vesperlysine A [23,31]. Our strategy relied on the latter approaches knowing that the extracted quantities of LW-1 might not be sufficient to obtain a much needed ^{13}C NMR and heteronuclear multiple quantum coherence (HMQC) spectra to resolve structural assignment ambiguities. In view of this unexpected difficulty and of the high budget for the proteolytic enzymes required to upscale the extraction of the acid-labile LW-1 from large quantities of collagen, it was decided to release the data in partial form.

The results of the NMR experiments in Figs. 6–8 suggest the presence of lysine in the structure of LW-1. Interestingly, the *triplet signal f* in the ^1H NMR at 4.4 ppm (Fig. 6) has also been observed in the proton NMR spectrum for various molecular cross-links isolated from different proteins including 2'-deoxyypyridinolone (lysyl pyridinolone) [29] and pentosidine [23] isolated from collagen; desmosine, isodesmosine and pentasine from elastin [30]; and vesperlysines A, B, C from AGE-BSA [33] as well as vesperlysine A from lens proteins [31]. In all cases, the signal was attributed to protons attached to the ϵ -carbon group of a lysine residue incorporated into a pyridinium ring type of structure through its ϵ -amino group.

In the present investigation, signals in the aromatic region of LW-1 (Fig. 6) resembled that of vesperlysine B [33]. However, unlike vesperlysine B [33], LW-1 showed no bathochromic shift in the spectra when the pH was varied (Fig. 5). Thus, there is no hydroxyl group attached to the aromatic ring as shown for vesperlysine B [33] and observed for many other glycation products. Quite puzzling are the sugar signals which we believe correspond to a glycosidically-linked sugar, implying thereby a biosynthetic step of the LW-1 precursors. Yet, still elusive is the nature of the second amino acid that is present, perhaps in peptide form in the molecule as suggested by the signals in the aliphatic region.

As for the relationship of LW-1 to total skin fluorescence and other fluorophores with similar excitation–emission wavelengths, the results show LW-1 as the single major peak in the HPLC chromatograms of enzymatic digests made from human insoluble skin collagen when monitored by fluorescence at ex/em 370/440 nm (Fig. 2). Levels (Fig. 11) significantly increased with age ($P < 0.0001$) and were accelerated by diabetes ($P < 0.0001$) and ESRD ($P = 0.021$). LW-1 accounted for $\sim 20\%$ of the total fluorescence in these digests. The rest of the autofluorescence was ubiquitously spread-out throughout the chromatogram in many minor peaks characterized by unresolved broadening and tailing effects (Fig. 2). These results are most likely due to incomplete digestion since LW-1 was proportional to the degree of digestion as assessed by repeating digestion from the same donor sample over time; i.e., the poorer, the smaller the LW-1 peak (unpublished results).

The protocol used here to sequentially and exhaustively digest the collagen with the series of enzymes listed in Fig. 1 is the same as previously used by us to measure glucosepane levels, whereby digestibility varied from 100% to 41% and showed an inverse relationship with age ($r = -0.19$, $P = 0.028$) between 8 and 90 years [17]. The digest used to isolate LW-1 in the present investigation was $\sim 62\%$ digested based upon hydroxyproline analysis before and after acid hydrolysis. In this, digestion of human collagen has always been problematic [34] mainly due to the accumulation of a host of post-translational modifications which increase with age and are accelerated by diabetes and renal disease [35]. These modifications are known to increase enzyme resistance to proteolytic digestion. A further challenge making it difficult to get complete digestion has to do with the structural make-up of triple-helical collagen; namely, the gly-x-y basic repeating unit of collagen, its high content of proline and hydroxyproline, and the presence of lysyl oxidase-derived physiological cross-links occurring in development, growth, and maturation [36].

A further observation made here is that the bulk of the hydroxyproline, used as a marker for collagen, tended to dissociate from the bulk of the highly fluorescent material containing LW-1 when the C18 clean-up column was used (Fig. 3). A similar observation has previously been made by us in the chromatography of enzymatic digests of human dura mater [37]. Since amino acid analysis of this material [37] showed profile characteristics for type I collagen [38]; i.e., high in glycine and alanine, we tentatively speculated that the fluorescence including LW-1 was associated with the telopeptide (nonhelical) region of collagen which is reportedly low in the α -imino acids [39]. However, this is doubtful for several reasons. First, nonenzymatic glycation is hypothesized and likely to be random along the collagen molecule at accessible residues [40] with reportedly preferential glycation sites [41]. Second, most if not all lysine residues of the $\alpha 1\text{C}$, $\alpha 1\text{N}$, and $\alpha 2\text{N}$ -telopeptide domains for type I collagen [42] from skin are thought to be tied-up in the physiological cross-linking process involving lysyl oxidase [43] ($\alpha 2\text{C}$ -telopeptide does not contain lysine [42]). Thus, it is unlikely that the telopeptides are important sites for LW-1 formation.

In spite of our current inability to propose a comprehensive structure for LW-1, several arguments support its critical and novel role as an important biomarker of cardiovascular risk in diabetes and ESRD. First, the above data show that LW-1 was the major component of the collagen-linked fluorescence, suggesting it is likely the major contributor of skin autofluorescence that is strong clinical predictor of cardiovascular morbidity and mortality in diabetes and ESRD. Second, and most excitingly, the finding that LW-1 was abnormally elevated in individuals dying without diabetes and ESRD but with severe lung disease suggests that it may be a marker of tissue hypoxia. However, such suggestion is presently speculative and further studies are needed in its investigation. Such finding could have broad implications since hypoxia has emerged as an

important pathological process in many diseases. In retrospect, the rapid increase in LW-1 in some nondiabetic individuals to a level equivalent to diabetics is rather perplexing and might suggest that LW-1 is not a glycation product.

Protein-link fluorescence has commonly been used as a marker and measure of advanced glycation *in vivo* mainly due to its high sensitivity and ease of measurement. However, it has also been frequently criticized for this purpose, most notably because of its nonspecificity since its formation can occur through reactions other than with sugars, especially lipids [44]. Second, proteins other than collagen are also modified by the Maillard reaction and show fluorescence [45]. Thus, there is a pragmatic interest in elucidating what these fluorescent structures are, as attempted in this study.

An additional issue concerns the relative importance and contribution of fluorescent vs. nonfluorescent molecules to the nonenzymatic cross-linking of collagen *in vivo*. In retrospect, many years ago, it was speculated that most of them must be relatively nonfluorescent, and perhaps colorless compounds; otherwise, they would be more apparent in the absorbance and fluorescence spectrum of the protein [46]. Furthermore, the fluorescent molecules which were identified at that time were concluded not to be present at sufficient levels to have any significant impact on the physical and chemical properties of collagen [46].

In regard to these issues, LW-1 is a fluorescent molecule similar to pentosidine but with fluorescent maxima at longer wavelengths; i.e., ex/em 348/463 vs. 335/385 nm, respectively, and comparable to LW fluorescence measured by the AGE Reader (see Introduction). Fluorescence between these two molecules does not overlap when quantified by analytical HPLC (see Results). Pentosidine is acid-stable and widely used as a marker to correlate the changes in the properties of collagen by glycation, yet it is a minor cross-link, averaging only about 1 molecule per 100 triple-helical collagen molecules. In comparison, the acid-labile glucosepane is a nonfluorescent glycation product and collagen cross-link with levels increasing up to ~2 nmol/mg collagen in insoluble skin collagen of old nondiabetic individuals and further increased up to ~4.3 nmol/mg in some diabetic patients [17]. These numbers translates into ~20–50 glucosepane molecules per 100 triple-helical collagen molecules in nondiabetic and diabetic individuals, respectively, which is sufficient to induce between a 30- and 45-fold decrease in collagen digestibility in diabetic skin collagen according to the results by Vater et al. [47]. In contrast, LW-1 is acid-labile and presently has not been established as a collagen cross-link since its structure is only partially known. However, as shown in Fig. 3, levels increased up to ~1–3 nmol/mg collagen in skin digests from nondiabetic and diabetic-ESRD patients, respectively. Thus, LW-1 is unexpectedly a major modification of collagen.

An important conclusion of this work is the critical importance to fully elucidate the structure of LW-1 and carry out studies on its clinical and biological significance. Currently, the single limiting factor is the costly upscale of the production of LW-1 from human collagen, such that not only a ¹³C-spectrum can be obtained, but sufficient material will be available for partial hydrolysis and study of its individual subcomponents. Perhaps and hopefully the current available data will provide clues to investigators who may have encountered similar data in their work.

Acknowledgments

The authors thank Dr. Beryl J. Ortwerth (Mason Eye Institute, University of Missouri, Columbia, MO) for the gifts of K2P and ST29; Dr. Marcus Glomb (Institute for Food Chemistry, Martin Luther University, Halle, Germany) for providing a free sample of argpyrimidine; the late Dr. Larry Sayre for providing ONE-pyrrole

(Department of Chemistry, Case Western Reserve University, Cleveland, OH); Dr. A. Daniel Jones (Department of Biochemistry & Molecular Biology and Department of Chemistry, Michigan State University, East Lansing, MI) in helping coordinate high resolution mass analysis at the Research Technology Support Facility (RTSF) at Michigan State University. Human skin tissue were obtained either from the Tissue Procurement Facility at University Hospitals Case Medical Center (Cleveland, OH) or from the National Disease Research Interchange (NDRI, Philadelphia, PA). This research was supported by National Institutes of Health (NIH) Grants R21 DK-79432 to D.R.S. and AG-18436 to V.M.M.

Appendix A. Supplementary data

Supplementary data associated with this article can be found, in the online version, at doi:10.1016/j.abb.2009.10.013.

References

- [1] V.M. Monnier, R.R. Kohn, A. Cerami, Proc. Natl. Acad. Sci. USA 81 (1984) 583–587.
- [2] V.M. Monnier, V. Vishwanath, K.E. Frank, C.A. Elemts, P. Dauchot, R.R. Kohn, N. Engl. J. Med. 314 (1986) 403–408.
- [3] V.M. Monnier, O. Bautista, D. Kenny, D.R. Sell, J. Fogarty, W. Dahms, P.A. Cleary, J. Lachin, S. Genuth, DCCT Collagen Ancillary Study Group, Diabetes 48 (1999) 870–880.
- [4] V.M. Monnier, O. Bautista, P.A. Cleary, D.R. Sell, S. Genuth, DCCT/EDIC Research Group, Diabetes 53 (Suppl. 2) (2004) A77–A78.
- [5] E.G. Gerrits, H.L. Lutgers, N. Kleefstra, R. Graaff, K.H. Groenier, A.J. Smit, R.O. Gans, H.J. Bilo, Diabetes Care 31 (2008) 517–521.
- [6] H.L. Lutgers, R. Graaff, T.P. Links, L.J. Ubink-Veltmaat, H.J. Bilo, R.O. Gans, A.J. Smit, Diabetes Care 29 (2006) 2654–2659.
- [7] J.D. Maynard, M. Rohrscheib, J.F. Way, C.M. Nguyen, M.N. Ediger, Diabetes Care 30 (2007) 1120–1124.
- [8] M. Monami, C. Lamanna, F. Gori, F. Bartalucci, N. Marchionni, E. Mannucci, Diabetes Res. Clin. Pract. 79 (2007) 56–60.
- [9] B. Conway, J. Wong, M. Ediger, T. Orchard, Sixty-eighth Scientific Sessions of the American Diabetes Association, 2008, Abstract 997-P.
- [10] J.W. Hartog, A.P. de Vries, H.L. Lutgers, R. Meerwaldt, R.M. Huisman, W.J. van Son, P.E. de Jong, A.J. Smit, Ann. NY Acad. Sci. 1043 (2005) 299–307.
- [11] E.G. Gerrits, A.J. Smit, H.J. Bilo, Nephrol. Dial. Transplant 24 (2009) 710–713.
- [12] H. Ueno, H. Koyama, S. Tanaka, S. Fukumoto, K. Shinohara, T. Shoji, M. Emoto, H. Tahara, R. Kakiya, T. Tabata, T. Miyata, Y. Nishizawa, Metabolism 57 (2008) 1452–1457.
- [13] A.S. Januszewski, N. Sachithanandan, C. Karschimkus, D. O'Neal, N. Alkatib, J. Best, K. Rowley, A.J. Jenkins, in: Ninth International Symposium on the Maillard Reaction, Munich, Germany, 2007, Abstract SVI-05.
- [14] R. Meerwaldt, J.W. Hartog, R. Graaff, R.J. Huisman, T.P. Links, N.C. den Hollander, S.R. Thorpe, J.W. Baynes, G. Navis, R.O. Gans, A.J. Smit, J. Am. Soc. Nephrol. 16 (2005) 3687–3693.
- [15] J. Blackwell, K.M. Katika, L. Pilon, K.M. Dipple, S.R. Levin, A. Novovong, J. Biomed. Opt. 13 (2008) 014004.
- [16] R. Meerwaldt, T.P. Links, R. Graaff, K. Hoogenberg, J.D. Lefrandt, J.W. Baynes, R.O. Gans, A.J. Smit, Diabetologia 48 (2005) 1637–1644.
- [17] D.R. Sell, K.M. Biemel, O. Reihl, M.O. Lederer, C.M. Strauch, V.M. Monnier, J. Biol. Chem. 280 (2005) 12310–12315.
- [18] S. Moore, W.H. Stein, J. Biol. Chem. 211 (1954) 907–913.
- [19] C.R. Hamlin, R.R. Kohn, Biochim. Biophys. Acta 236 (1971) 458–467.
- [20] O.K. Argirov, B. Lin, P. Olesen, B.J. Ortwerth, Biochim. Biophys. Acta 1620 (2003) 235–244.
- [21] I.N. Shipanova, M.A. Glomb, R.H. Nagaraj, Arch. Biochem. Biophys. 344 (1997) 29–36.
- [22] R. Cheng, Q. Feng, O.K. Argirov, B.J. Ortwerth, J. Biol. Chem. 279 (2004) 45441–45449.
- [23] D.R. Sell, V.M. Monnier, J. Biol. Chem. 264 (1989) 21597–21602.
- [24] G. Xu, Y. Liu, L.M. Sayre, J. Org. Chem. 64 (1999) 5732–5745.
- [25] W.-H. Zhang, J. Liu, G. Xu, Q. Yuan, L.W. Sayre, Chem. Res. Toxicol. 16 (2003) 512–523.
- [26] K. Nakamura, Y. Nakazawa, K. Ienaga, Biochem. Biophys. Res. Commun. 232 (1997) 227–230.
- [27] D. Fujimoto, T. Moriguchi, T. Ishida, H. Hayashi, Biochem. Biophys. Res. Commun. 84 (1978) 52–57.
- [28] Z. Deyl, K. Macek, M. Adam, O. Vancíková, Biochim. Biophys. Acta 625 (1980) 248–254.
- [29] T. Ogawa, T. Ono, M. Tsuda, Y. Kawanishi, Biochem. Biophys. Res. Commun. 107 (1982) 1252–1257.
- [30] B. Starcher, G. Cook, P. Gallop, E. Hensen, B. Shoulders, Connect. Tissue Res. 16 (1987) 15–25.
- [31] F. Tessier, M. Obrenovich, V.M. Monnier, J. Biol. Chem. 274 (1999) 20796–20804.

- [32] M.E. Bollard, S. Garrod, E. Holmes, J.C. Lindon, E. Humpfer, M. Spraul, J.K. Nicholson, *Magn. Reson. Med.* 44 (2000) 201–207.
- [33] K. Nakamura, Y. Nakazawa, K. Ienaga, *Biochem. Biophys. Res. Commun.* 232 (1997) 227–230.
- [34] C.R. Hamlin, J.H. Luschin, R.R. Kohn, *Exp. Gerontol.* 13 (1978) 403–414.
- [35] N. Verzijl, J. DeGroot, S.R. Thorpe, R.A. Bank, J.N. Shaw, T.J. Lyons, J.W. Bijlsma, F.P. Lafeber, J.W. Baynes, J.M. TeKoppele, *J. Biol. Chem.* 275 (2000) 39027–39031.
- [36] A.J. Bailey, *Mech. Ageing Dev.* 122 (2001) 735–755.
- [37] D.R. Sell, V.M. Monnier, *Connect. Tissue Res.* 19 (1989) 77–92.
- [38] A. Asghar, R.L. Henrickson, *Adv. Food Res.* 28 (1982) 231–372.
- [39] J.D. Brady, S.P. Robins, *J. Biol. Chem.* 276 (2001) 18812–18818.
- [40] A.J. Bailey, R.G. Paul, L. Knott, *Mech. Ageing Dev.* 106 (1998) 1–56.
- [41] K.M. Reiser, M. Amigable, J.A. Last, *J. Biol. Chem.* 267 (1992) 24207–24216.
- [42] J.P. Malone, A. Veis, *Biochemistry* 43 (2004) 15358–15366.
- [43] N.C. Avery, T.J. Sims, A.J. Bailey, *Methods Mol. Biol.* 522 (2009) 103–121.
- [44] K. Kikugawa, M. Beppu, *Chem. Phys. Lipids* 44 (1987) 277–296.
- [45] S.E. Hormel, D.R. Eyre, *Biochim. Biophys. Acta* 1078 (1991) 243–250.
- [46] J.W. Baynes, *Diabetes* 40 (1991) 405–412.
- [47] C.A. Vater, E.D. Harris Jr., R.C. Siegel, *Biochem. J.* 181 (1979) 639–645.